



# A new test specimen for the determination of the field of view of small-area X-ray photoelectron spectrometers

Jörg M. Stockmann<sup>1</sup> | Jörg Radnik<sup>1</sup> | Sebastian Bütfisch<sup>2</sup> | Ingo Busch<sup>2</sup> | Thomas Weimann<sup>3</sup> | Cristiana Passiu<sup>4</sup> | Antonella Rossi<sup>4,5</sup> | Wolfgang E.S. Unger<sup>1</sup>

<sup>1</sup>Surface Analysis and Interfacial Chemistry, Bundesanstalt für Materialforschung und -prüfung, Berlin, Germany

<sup>2</sup>Scanning Probe Metrology, Physikalisch-Technische Bundesanstalt, Braunschweig, Lower Saxony, Germany

<sup>3</sup>Nanostructuring and Clean Room Center Infrastructure, Physikalisch-Technische Bundesanstalt, Braunschweig, Lower Saxony, Germany

<sup>4</sup>Department of Materials, ETH Zürich, Zürich, Switzerland

<sup>5</sup>Department of Chemical and Geological Sciences, University of Cagliari, Cagliari, Italy

## Correspondence

Jörg M. Stockmann, Surface Analysis and Interfacial Chemistry, Bundesanstalt für Materialforschung und -prüfung, Berlin, Germany.

Email: joerg-manfred.stockmann@bam.de

Small-area/spot photoelectron spectroscopy (SAXPS) is a powerful tool for the investigation of small surface features like microstructures of electronic devices, sensors or other functional surfaces, and so forth. For evaluating the quality of such microstructures, it is often crucial to know whether a small signal in a spectrum is an unwanted contamination of the field of view (FoV), defined by the instrument settings, or it originated from outside. To address this issue, the  $d_{80/20}$  parameter of a line scan across a chemical edge is often used. However, the typical  $d_{80/20}$  parameter does not give information on contributions from the long tails of the X-ray beam intensity distribution or the electron-optical system as defined by apertures. In the VAMAS TWA2 A22 project "Applying planar, patterned, multi-metallic samples to assess the impact of analysis area in surface-chemical analysis," new test specimen was developed and tested. The here presented testing material consists of a silicon wafer substrate with an Au-film and embedded Cr circular and square spots with decreasing dimensions from 200  $\mu\text{m}$  down to 5  $\mu\text{m}$ . The spot sizes are traceable to the length unit due to size measurements with a metrological SEM. For the evaluation of the FoV, we determined the Au4f intensities measured with the center of the FoV aligned with the center of the spot and normalized to the Au4f intensity determined on the Au-film. With this test specimen, it was possible to characterize, as an example, the FoV of a Kratos AXIS Ultra DLD XPS instrument.

## KEY WORDS

field of view, reference material, selected area XPS, small-area XPS, small-spot XPS

## 1 | INTRODUCTION

Imaging XPS (iXPS) has been available on XPS instruments since 1990s<sup>1</sup> with a spatial resolution in the lower micrometer range. Recent industrial applications and actual research issues are dealing with small micrometer-sized surface features, which determine the functionality of devices thereon. The diversity of applications ranges from solar cells, microelectronics and optoelectronics, biological

arrays, corrosion, tribology, catalysis to sensor-on-chip and sensor-on-lab systems.<sup>2</sup> Additionally, for combinatorial approaches, iXPS can be used.<sup>3</sup> iXPS is combined often with SAXPS. A chemical image or map of the surface is generated. In those images or maps, regions can be defined and measured to obtain qualitative and quantitative chemical information, for example, chemical composition. Different methods for SAXPS are described: (i) limited X-ray irradiated area based, selection of the area by electron (ii) before or (iii) after the entrance of the

This is an open access article under the terms of the Creative Commons Attribution License, which permits use, distribution and reproduction in any medium, provided the original work is properly cited.

© 2020 The Authors. Surface and Interface Analysis published by John Wiley & Sons Ltd

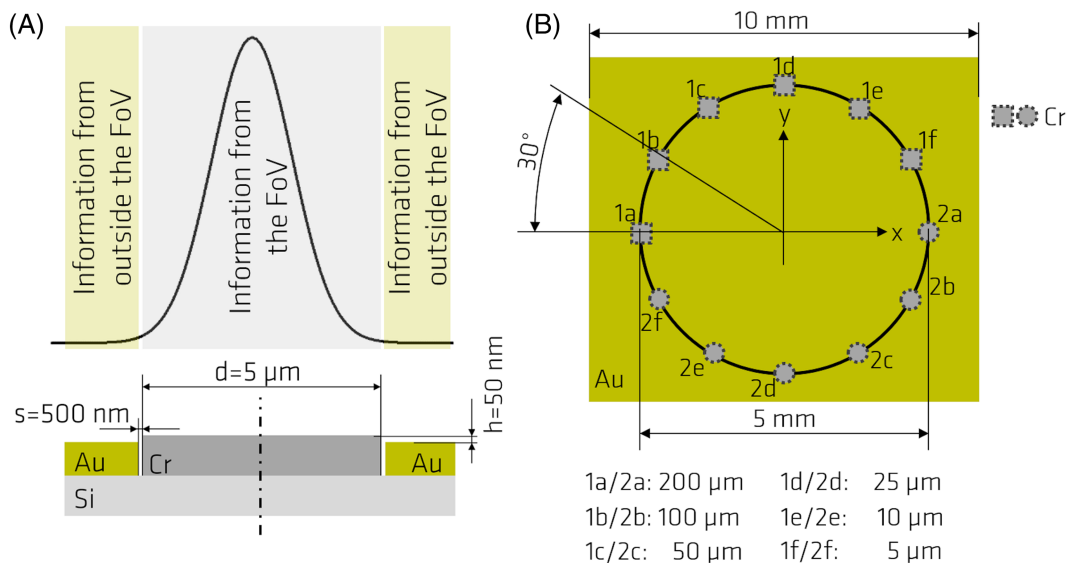


**FIGURE 1** A, Top: the tails of the X-ray beam shapes lead to contribution from outside the field of view (FoV); bottom: section across the Cr circular spot of 5 μm diameter. B, Target design of test structure. Layout and dimensions of the test structures on the test specimen

ejected electrons in the electron analyzer or (iv) image dissection in the analyzer.<sup>4</sup> Regardless of the method, it is often unclear if a specific peak in the spectrum arises from a contamination of a surface feature from an area outside the region of interest.<sup>5,6</sup> For describing the lateral resolution typically, the  $d_{80/20}$  parameter is used.<sup>7,8</sup> It is determined by the imaging of a sharp straight edge. From a line profile perpendicular to the edge, the distance between  $D_{80}$  (80 % of the intensity) and  $D_{20}$  (20 % of the intensity) can be taken as a measure of sharpness. It must be noted that this quantity does not consider long tails of the X-ray beam intensity distribution or of the electron-optical system, which can lead to contributions outside the FoV that is shown in Figure 1A. To be sure, small surface features can be analyzed with clear smaller beam apertures,<sup>9</sup> but this is challenging, for various reasons. Due to these reasons, a reliable and traceable determination of the FoV becomes highly relevant and requires an appropriate test specimen<sup>10</sup>; see Figure 1B. There is a need for control of the FoV by using such test specimens for XPS users as well as instrument manufacturers.

## 2 | EXPERIMENTAL

### 2.1 | Test specimen and micrometer structures thereon

Useful test structures used to characterize the FoV are Cr squares and circular spots, which are embedded in a 100-nm-thick Au-film arranged on a circle with a diameter  $D = 5$  mm. This target design is manufactured on a  $10 \times 10$  mm<sup>2</sup> silicon substrate by Physikalisch-Technische Bundesanstalt (PTB) using e-beam technology. The test structures have dimensions/diameters from 200 μm down to 5 μm. Between the Au-film and the test structures is a small spacing  $s$ ; see Figure 1A.

### 2.2 | SEM imaging and profilometry for validation of features on the test specimen

For quality control reasons, the test sample was investigated with scanning electron microscopy (SEM) and profilometry. The structure dimensions  $d$  and  $s$  were determined as well as their height  $h$ . All SEM measurements were carried out with a ZEISS Supra 40 with a Schottky field emitter cathode using 20 keV as excitation energy and different magnifications for the test structures. A conventional secondary-electron detector (SE) was utilized to image the test structures, and an in-lens detector was utilized to measure the spacing  $s$ ; see Figure S3b. The image magnification at the SEM was calibrated by using the dedicated structure 1 μm pitch of the length reference material "S 1995" (Plano GmbH, Wetzlar, Germany) accompanied by a PTB certificate stating traceability to the length unit. The profilometry measurements were carried out mechanically with a BRUKER Dektak XT profiler, and the test structures were imaged with an optical microscope. The device is calibrated with a reference measurement on a traceable step height standard: VLSI Standards Inc. USA, traceable on SI Units (NIST), certified height: 429.3 nm ± 3.6 nm, serial number and certificate: 3421-11-20. The measurement velocity was turned to slow mode, the measuring distance was extended to 5 to 6 times the structure dimension, and data points were taken every 0.4 μm. For accurate measurements of the smallest Cr circular spot, multiple positioning steps were applied to achieve correct determination of the diameters and heights or depths.

### 2.3 | XPS measurements

All XPS spectroscopic as well as imaging measurements were performed with an AXIS Ultra DLD photoelectron spectrometer manufactured by Kratos Analytical (Manchester, UK). XP-spectra were

recorded using monochromatized aluminum K $\alpha$  radiation for excitation, at a pressure in the UHV region (between  $10^{-8}$  and  $10^{-9}$  mbar). The electron emission angle was  $0^\circ$ , and the source-to-analyzer angle was  $60^\circ$ . The binding energy (BE) scale of the instrument was calibrated following a Kratos procedure, which is based on ISO 15472 BE data. Survey and narrow scan spectra were taken by setting the lens mode to "field of view 2" (FoV2, small-spot mode). The pass energy was set to 160 eV for survey and for narrow scan spectra. The survey spectra were recorded with a step size of 1 eV and the narrow scan spectra with a step size of 0.1 eV. Four different apertures (110, 55, 27, and 15  $\mu\text{m}$ ) were applied to vary the area of analysis. Parallel imaging was performed with the FoV2 lens mode and the position of the iris for best lateral resolution ("imaging high resolution"). The focus was determined according to a procedure provided by Kratos (see Supporting Information and Figure S2). The spectra were quantified with the CasaXPS-software version 2.3.16 Pre-rel 1.4, and C1s peak BE is referred to 285.0 eV. For the normalization process of the Au4f intensities on Cr circular spots, the peak areas of the Au4f intensities on Cr circular spots were considered in relation to the peak areas of the Au4f intensities from the Au-film. Hence, fixed BE limits 80 to 92 eV were applied for the Au4f doublet peak area determination.

### 3 | RESULTS AND DISCUSSION

#### 3.1 | SEM

All test structures were imaged, and their dimensions were determined. The largest deviation, of 0.6  $\mu\text{m}$ , is between the nominal value of the 100- $\mu\text{m}$  Cr square spot and the measured value. The spacings between the Au-film edge and Cr-structure were between 0.18 and 0.21  $\mu\text{m}$ ; see Figure S3 and Table 1. The main uncertainties of the length measurements are due to the pixel sizes for the SE measurements and the not sharp edges of the structures for the in-lens measurements. All test structures comply with the requirements, and the deviations from the theoretical layout (nominal value) are relatively small. The deviations in Table 1 are the overall measurement uncertainties.

#### 3.2 | Profilometry

The difference in the height  $h$  between the Au-film and the Cr circular spots is around 25 nm, see Table S1, which ensures a correct sample

alignment on the z direction via parallel imaging mode of the Kratos AXIS Ultra DLD instrument. The real design of the test structures is significantly better than the target design, because the spacing  $s$  and the difference in height  $h$  are smaller than the recommended values; see Supporting Information-profilometry and Table S1.

#### 3.3 | XPS

The measurement routine to characterize the FoV follows Baer's and Engelhard's<sup>11</sup> and Scheithauer's approaches.<sup>12</sup> Figure 2 shows XPS images of four Cr circular spots (200 to 25  $\mu\text{m}$ ).

Using our Cr test structures, it is possible to determine the intensity contribution from outside the FoV to the XPS Au4f signal in the spectra. Running the routine, three measurements were needed. In the first step, images of the test structures were taken at the BE where the maximum of the Au4f<sub>7/2</sub> peak intensity had been determined before. In the second step, the measurement of the Au4f peak intensity  $I_{\text{Au}}^{\text{circle}}$  with the analyzer axis set to the center of the Cr circular spot was measured (with three sweeps, repeated five times). In the third step, the measurement of the Au4f peak intensity  $I_{\text{Au}}^{\text{reference}}$  was measured on the Au-film at least 500  $\mu\text{m}$  away from the respective Cr circular spot under the same conditions as in Step 2. All steps were repeated for each device aperture using the same set of circular spots. After finishing the measurements in Steps 2 and 3, all Au4f peak intensities were determined by peak fitting in terms of peak areas, and average values were calculated. Subsequently, the Au4f area ratio values were calculated by calculating the quotient of the average intensity of  $I_{\text{Au}}^{\text{circle}}$  and the average intensity of  $I_{\text{Au}}^{\text{reference}}$  for each circle and set beam aperture. As a result, the calculated Au4f area ratio value is the part that comes from outside the FoV and contributes to the overall intensity. At this point, the Au4f-ratio-aperture diagram could be prepared; see Figure 3. The abscissa shows the apertures of the Kratos AXIS Ultra DLD instrument, and the ordinate shows the Au4f area ratio  $I_{\text{Au}}^{\text{circle}}/I_{\text{Au}}^{\text{reference}}$ . In general, the smaller the Cr circular spots, the more intensity information from outside the nominal FoV was found in the measured spectra. If the instrument's aperture becomes small, the signal contribution from outside the nominal FoV is decreased. For all aperture diameters, the major part of the intensity for the circular spot of 25  $\mu\text{m}$  diameter originated from outside the circular spot. Addressing the circular spot of 25  $\mu\text{m}$  diameter using apertures from 27 up to 110  $\mu\text{m}$  reveals large  $I_{\text{Au}}^{\text{circle}}/I_{\text{Au}}^{\text{reference}}$  ratios between 90 % and 100 %. Only with the 15  $\mu\text{m}$

**TABLE 1** Measurement of dimensions for test structures and spacings between Au-film edge and Cr-structure

Nominal value/ $\mu\text{m}$	Cr square length/ $\mu\text{m}$	Spacing $s/\mu\text{m}$	Cr circular spot diameter/ $\mu\text{m}$	Spacing $s/\mu\text{m}$
200	$200.1 \pm 0.30$	$0.22 \pm 0.01$	$200.3 \pm 0.35$	$0.19 \pm 0.01$
100	$99.4 \pm 0.16$	$0.21 \pm 0.01$	$99.8 \pm 0.19$	$0.20 \pm 0.01$
50	$49.4 \pm 0.08$	$0.21 \pm 0.01$	$49.8 \pm 0.05$	$0.20 \pm 0.01$
25	$24.7 \pm 0.04$	$0.20 \pm 0.01$	$24.6 \pm 0.09$	$0.18 \pm 0.01$
10	$9.6 \pm 0.02$	$0.18 \pm 0.01$	$9.6 \pm 0.02$	$0.19 \pm 0.01$
5	$4.6 \pm 0.01$	$0.19 \pm 0.01$	$4.6 \pm 0.01$	$0.18 \pm 0.01$

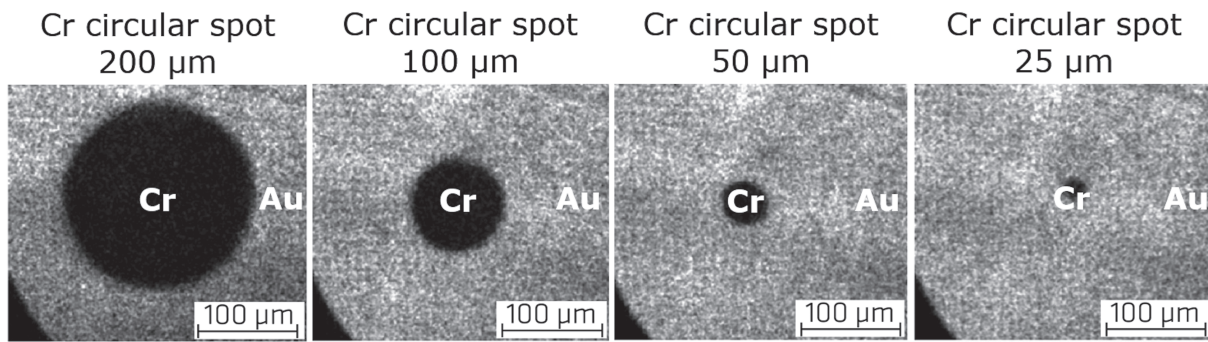
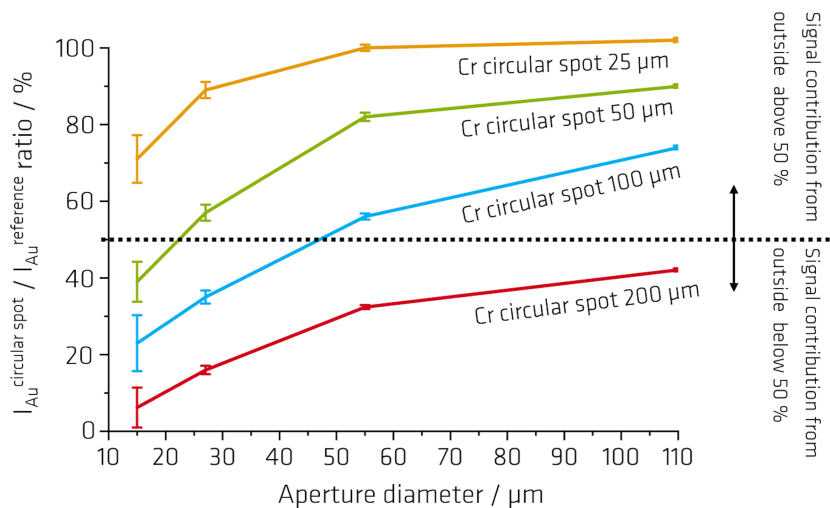


**FIGURE 2** XPS images of four different Cr circular spots taken at 83.6 eV binding energy (BE) and using the KRATOS FoV2 parallel imaging mode

**FIGURE 3**  $I_{\text{Au}}^{\text{circle}}/I_{\text{Au}}^{\text{reference}}$  ratios measured with the Cr pattern shown in Figure 2 as a function of the aperture size of the Kratos instrument used in FoV2 parallel imaging mode and taken at 83.6 eV binding energy (BE). The Cr spot diameter is a parameter in the experiment



aperture, the signal contribution from outside the nominal FoV defined by that aperture is below 80 %. The relevant information derived from the graphs in Figure 3 is that apertures smaller than 30 % of the structure dimensions of the analyzed spot lead to a contribution below 50 % from outside the nominal FoV defined by the used aperture. For the 25- $\mu\text{m}$  circular spot, no suitable aperture is available, which can prove the 30 % statement. It must be noted that these results are only valid for our instrument. For other XPS instruments, with other electron optics or with a focused X-ray beam, the Au4f ratio diagrams can vary and should be determined individually.

#### 4 | CONCLUSION AND OUTLOOK

For microstructured surfaces, it is crucial to know if a small signal obtained in a “small-spot” or “small-area” XPS measurement originated from outside or inside the region of interest. Only with the help of appropriate test specimen carrying structures that allow the determination of the FoV of the instrument can be directly addressed this question. Our results emphasize the importance of such investigations. The FoV is usually several times larger than the aperture of the instrument. With the procedure and test specimen presented here, it

is possible to quantify the influence of undesired contributions from outside the region of interest. Such knowledge of the relation between the aperture size and the applied FoV required for an analysis of a structure of certain dimensions on the sample's surface is needed. To avoid unwanted signal contributions from outside a structure, for example, in quantitative surface chemical analysis, due to the wings in the profile of the X-ray beam shape, the utilized aperture or spot size of the Kratos AXIS Ultra DLD XPS instrument must be approximately three times smaller than the dimension of the analyzed structure. For other XPS devices with different X-ray beam geometries and electron optics, the results will be different. It is beyond question that a determination of the correlation between instruments settings and the FoV is necessary to obtain credible “small-spot” or “small-area” measurements. Additionally, two other quantities can be determined with the presented test specimen: the sizes of the spots are traceable due to the measurements of the structures with a metrological SEM and can be used to determine the length scale established in a XPS image, and furthermore, astigmatism can be determined by looking at the Cr squares.

A future task is the optimization of the sample layout based on feedback of the participants of the VAMAS TWA2 A22 project and the production of the final specimen for sale. An aging study of the

used Cr in Au on the test specimen is also planned. Finally, the preparation of an ISO standard derived on outcome of VAMAS TWA2 A22 project is on the agenda of ISO TC 201.

## ACKNOWLEDGMENTS

The authors thank Dr. U. Mansfeld for SEM and Dipl.-Ing. M. Weise for profilometry measurements. We thank also international colleagues who participated in the VAMAS TWA2 A22 project for feedback on the performance and design of the test specimen.

## ORCID

Jörg M. Stockmann  <https://orcid.org/0000-0001-5856-5504>

Jörg Radnik  <https://orcid.org/0000-0003-0302-6815>

Wolfgang E.S. Unger  <https://orcid.org/0000-0002-7670-4042>

## REFERENCES

1. Seah MP, Smith GC. Concept of an imaging XPS system. *Surf Interface Anal.* 1988;11(1–2):69–79.
2. Morgan DJ. Imaging XPS for industrial applications. *Journal of Electron Spectroscopy and Related Phenomena.* 2019;231:109–117.
3. Eglin M, Rossi A, Spencer ND. X-ray photoelectron spectroscopy analysis of tribostressed samples in the presence of ZnDTP: a combinatorial approach. *Tribology Letters.* 2003;15(3):199–209.
4. Drummond IW, Cooper TA, Street FJ. Four classes of selected area XPS (SAXPS): an examination of methodology and comparison with other techniques. *Spectrochimica Acta Part B: Atomic Spectroscopy.* 1985;40(5–6):801–810.
5. Yates K, West RH. Small area x-ray photoelectron spectroscopy. *Surf Interface Anal.* 1983;5(5):217–221.
6. Forsyth NM, Coxon P. Use of parallel imaging XPS to perform rapid analysis of polymer surfaces with spatial resolution > 5 μm. *Surf Interface Anal.* 1994;21(6–7):430–434.
7. ISO/TR 19319: 2013 ISO 18516:2006, Surf. Chem. Anal. - Auger electron spectroscopy and X-ray photoelectron spectroscopy - Determination of lateral resolution to be replaced by ISO 18516: 2019, Surface chemical analysis - Determination of lateral resolution and sharpness in beam-based methods.
8. Senoner M, Unger WES. Summary of ISO/TC 201 technical report: ISO/TR 19319: 2013—surface chemical analysis - fundamental approaches to determination of lateral resolution and sharpness in beam-based methods. *Surf Interface Anal.* 2013;45(9):1313–1316.
9. ASTM Standard : E1217-11 “Determination of Specimen Area Contributing to the Detected Signal in Auger Electron Spectrometers and Some X-Ray Photoelectron Spectrometers” 2019 Announced book of ASTM standards, Vol 3.06 (ASTM Internationalo, West Conshohocken)
10. Passiu C, Rossi A, Bernard L, et al. Fabrication and microscopic and spectroscopic characterization of planar, bimetallic, micro-and nanopatterned surfaces. *Langmuir.* 2017;33(23):5657–5665.
11. Baer D R, and Engelhard M H. "Approach for determining area selectivity in small-area XPS analysis. *Surf Interface Anal.* (2000);29: 766–772.
12. Scheithauer U. Quantitative lateral resolution of a quantum 2000 X-ray microprobe. *Surf Interface Anal.* 2008;40(3-4):706–709.

## SUPPORTING INFORMATION

Additional supporting information may be found online in the Supporting Information section at the end of this article.

**How to cite this article:** Stockmann JM, Radnik J, Bütfisch S, et al. A new test specimen for the determination of the field of view of small-area X-ray photoelectron spectrometers. *Surf Interface Anal.* 2020;52:890–894. <https://doi.org/10.1002/sia.6831>